Time-Accurate Schemes for Computing Two- and Three-Dimensional Viscous Fluxes on Unstructured Dynamic Meshes

Bruno Koobus, Charbel Farhat

INSTITUT NATIONAL DE RECHERCHE EN INFORMATIQUE ET EN AUTOMATIQUE

Time-Accurate Schemes for Computing Two- and Three-Dimensional Viscous Fluxes on Unstructured Dynamic Meshes

Bruno KOOBUS and Charbel FARHAT.

N° 2823

Mars 1996

PROGRAMME 6

ISSN 0249-6399

INRIA
SOPHIA ANTIPOLIS

Time-Accurate Schemes for Computing Two- and Three-Dimensional Viscous Fluxes on Unstructured Dynamic Meshes

Bruno KOOBUS and Charbel FARHAT. *

Programme 6 — Calcul scientifique, modélisation et logiciel numérique
Projet SINUS

Rapport de recherche n ° 2823 — Mars 1996 — 14 pages

Abstract: Numerical simulations of viscous flow problems with complex moving boundaries commonly require the solution of the fluid equations on unstructured and deformable dynamic meshes. In this paper, we present a time-accurate methodology for computing the unsteady diffusive fluxes arising from such problems, and highlight its impact on the accuracy of the overall flow simulation. We illustrate this methodology with a viscous flow problem related to a supersonic aeroelastic application. The numerical schemes presented in this paper can be directly extended to the computation of turbulent flows on moving grids.

Key-words: Fluid Dynamics, Navier-Stokes equations, Moving boundaries, Unstructured meshes, Two- and Three-dimensional flows.

(Résumé : tsvp)

* Center for Aerospace Structure, University of Colorado, Campus Box 429, Boulder, CO 80309-0429, USA.

Schémas d'intégration précis en temps pour le calcul des flux visqueux bi- et tridimensionnels en maillages déformables non structurés

Résumé : La simulation numérique d'écoulements visqueux dans des domaines a frontières mobiles nécéssite en général la résolution des équations fluides sur des maillages déformables mobiles et non structurés. Dans ce rapport nous présentons une méthodologie d'intégration précise en temps pour le calcul des flux visqueux instationnaires dans de tels problèmes. On illustre cette étude avec la simulation d'un écoulement visqueux dans un cas de plaque oscillante supersonique. Les schémas numériques présentés dans ce rapport peuvent être directement étendus au cas d'écoulements turbulents en maillages déformables.

Mots-clé : Dynamique des Fluides, Equations de Navier-Stokes, Domaines déformables, Maillages non structurés, Ecoulements bi- et tridimensionnels.

Contents

1 Introduction

In the past two decades, the problem of computing unsteady flows around oscillating airfoils and wings has received considerable attention, especially from the computational aeroelasticity community [1, 2]. Early investigations of such problems have essentially focused on Euler flows, but laminar and turbulent viscous flows are often being considered nowadays [6].

When some of the fluid domain boundaries undergo a motion with a large amplitude, it becomes necessary to solve the flow equations on a moving and possibly deforming grid. Several approaches have been proposed for tackling such problems, among which we note two closely related methods: the dynamic meshes [3] and Arbitrary Lagrangian Eulerian (ALE) formulations [4, 5].

Whichever method is selected for solving the time-dependent fluid equations, it must preserve the trivial solution of a uniform flow field (in the absence of other boundary conditions, a uniform flow field is a solution of the Navier-Stokes equations). In [7, 8], the authors have shown that this property is verified only when the numerical scheme chosen for solving the flow problem, and the algorithm constructed for updating the mesh motion, satisfy a Geometric Conservation Law (GCL) that is similar in its principle to the GCL condition that was first pointed out in [9] for structured grids and finite difference schemes. However, because the GCL condition affects only the convective fluxes, many authors have emphasized the correct computation of these [10, 11, 12, 7], and little has been written about the time-accurate evaluation of the diffusive fluxes on unstructured dynamic meshes. The main objective of this paper is to fill this gap. For this purpose, its remainder is organized as follows.

In Section 2, we summarize the ALE formulation of the Navier-Stokes equations on moving grids. We discretize the convective fluxes by an unstructured finite volume method, and the diffusive ones by a P1 finite element approximation. In Section 3, we consider the problem of evaluating correctly the unsteady diffusive fluxes in two- and three-dimensional spaces. We derive a family of algorithms for time-integrating these fluxes on dynamic meshes, and analyze their time-accuracy. In Section 4, we apply these algorithms to the prediction of the unsteady supersonic viscous flow above a panel oscillating around its fundamental elastic mode. Finally, we conclude this paper in Section 5.

2 Formulation and discretization of the Navier-Stokes equations on dynamic meshes

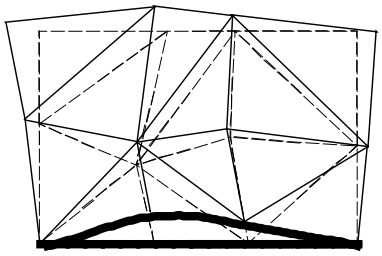

Figure 1: Deformable dynamic mesh

Let $\Omega(t) \subset \mathcal{R}^n$ $(n = 2,\ 3)$ be the flow domain of interest, and $\Gamma(t)$ be its moving and/or deforming boundary. We introduce a mapping function between $\Omega(t)$ where time is denoted by t and a grid point coordinates by x, and a reference configuration $\Omega(0)$ where time is denoted by θ and a grid point coordinates by ξ, as follows

$$x \ = \ x(\xi, \theta); \quad t = \theta \tag{1}$$

The ALE nondimensional conservative form of the Navier-Stokes equations describing viscous flows on dynamic meshes can be written as[7, 8]

$$\frac{\partial JW}{\partial t}|_\xi + J\nabla_x.\mathcal{F}^c(W, \dot{x}) = J\nabla_x.\mathcal{R}(W) \tag{2}$$
$$\mathcal{F}^c(W, \dot{x}) = \mathcal{F}(W) - \dot{x}W$$

where a dot superscript designates a time derivative, $J = det(dx/d\xi)$, $\dot{x} = \dfrac{\partial x}{\partial \tau}|_\xi$, (x, t), and (ξ, τ) are the grid point coordinates and time variable associated with the flow configuration at time t and a reference configuration, respectively, W is the fluid state vector, $\mathcal{F}^c$ denotes the ALE convective fluxes, and $\mathcal{R}$ the diffusive fluxes.

For two-dimensional flows, W, $\mathcal{F}$ and $\mathcal{R}$ are given by

$$W = \begin{pmatrix} \rho \\ \rho v_1 \\ \rho v_2 \\ E \end{pmatrix}$$

$$\mathcal{F}(W) = \begin{pmatrix} \mathcal{F}_1(W) \\ \mathcal{F}_2(W) \end{pmatrix} \quad , \quad \mathcal{R}(W) = \begin{pmatrix} \mathcal{R}_1(W) \\ \mathcal{R}_2(W) \end{pmatrix}$$

$$(\mathcal{F}_1(W), \mathcal{F}_2(W)) = \begin{pmatrix} \rho\vec{v}^t \\ \rho v_1 \vec{v}^t + p\vec{e}_1^t \\ \rho v_2 \vec{v}^t + p\vec{e}_2^t \\ (E+p)\,\vec{v}^t \end{pmatrix}$$

$$(\mathcal{R}_1(W), \mathcal{R}_2(W)) = \frac{\mu}{Rey} \begin{pmatrix} \vec{0}^t \\ (\sigma.\vec{e}_1)^t \\ (\sigma.\vec{e}_2)^t \\ (\sigma.\vec{v})^t + \dfrac{\gamma}{Pr}\nabla^t e \end{pmatrix}$$

where

$$\begin{aligned} &E = \rho e + \tfrac{1}{2}\rho\|\vec{v}\|^2 \\ &p = (\gamma-1)\rho e \\ &\sigma = \nabla\vec{v} + \nabla^t\vec{v} - \frac{2}{3}\nabla.\vec{v}I_d \\ &\vec{v} = (v_1, v_2)^t \\ &\gamma = \frac{c_p}{c_v} \\ &\vec{0} = (0,0)^t \\ &\vec{e}_1 = (1,0)^t \quad \text{and } \vec{e}_2 = (0,1)^t \end{aligned}$$

and ρ is the fluid density, p its pressure, e its specific internal energy, $\vec{v} = (v_1,\ v_2)$ its velocity vector, μ its laminar viscosity, γ its specific heat ratio, Rey the Reynolds number, Pr the Prandtl number, σ the stress tensor, I_d the identity matrix, and a t superscript designates the transpose of a vector.

We discretize Eq. (2) on a triangulation (two-dimensional problems) or a tetrahedral mesh (three-dimensional problems) from which we derive a dual mesh defined by control volumes or cells (Fig. 2).

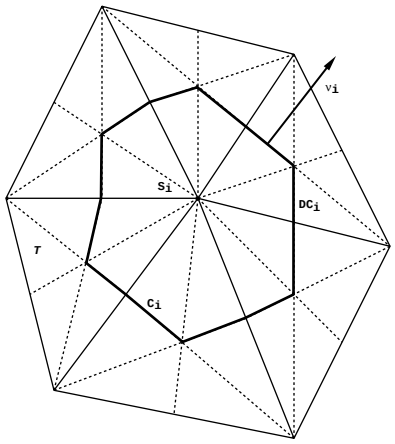

Figure 2: Control volume (unstructured two-dimensional mesh)

First, we integrate Eq. (2) over a reference cell $C_i(0)$ of the ξ space

$$\int_{C_i(0)} \frac{\partial JW}{\partial t}|_\xi d\Omega_\xi + \int_{C_i(0)} \nabla_x.\mathcal{F}^c(W,\dot{x})Jd\Omega_\xi = \int_{C_i(0)} \nabla_x.\mathcal{R}(W)Jd\Omega_\xi$$

Since the partial time derivative is evaluated at a constant ξ, we move it outside of the integral sign to obtain

$$\frac{d}{dt}\int_{C_i(0)} WJd\Omega_\xi + \int_{C_i(0)} \nabla_x.\mathcal{F}^c(W,\dot{x})Jd\Omega_\xi = \int_{C_i(0)} \nabla_x.\mathcal{R}(W)Jd\Omega_\xi \tag{3}$$

Next, we switch from the ξ reference space to the x space at time t and transform Eq. (3) into

$$\frac{d}{dt}\int_{C_i(t)} Wd\Omega_x + \int_{C_i(t)} \nabla_x.\mathcal{F}^c(W,\dot{x})d\Omega_x = \int_{C_i(t)} \nabla_x.\mathcal{R}(W)d\Omega_x \tag{4}$$

Finally, we integrate by parts the convective and diffusive fluxes, which leads to

$$\frac{d}{dt}\int_{C_i(t)} Wd\Omega_x + \int_{\partial C_i(t)} \mathcal{F}^c(W,\dot{x}).\vec{n}d\sigma = \int_{\partial C_i(t)} \mathcal{R}(W).\vec{n}d\sigma \tag{5}$$

where $\partial C_i(t)$ denotes the cell boundary.

Throughout this paper, we resolve the ALE convective fluxes by a suitable Reimann solver [13, 7, 12], and approximate the diffusive terms by piecewise linear finite elements. The resulting semi-discrete version of Eq. (5) is

$$\frac{d}{dt}(A_iW_i) + F_i(W,X,\dot{X}) = R_i(W,X) \tag{6}$$

where $A_i = \int_{C_i(t)} d\Omega_x$, W_i denotes the average value of W over the cell $C_i(t)$, F_i and R_i denote respectively the discretized ALE convective and diffusive fluxes, W is the vector formed by the collection of W_i, and X is the vector of time-dependent grid point positions. Various expressions of the flux approximation $F_i(W,X,\dot{X})$ can be found in [12, 7]. On the other hand, the discrete diffusive fluxes are simply given by

$$R_i(W,X) = \sum_{T,\ i\in T} \mathcal{R}(T).\vec{\nu}_{i,T} \tag{7}$$

where T is a triangle in two-dimensional problems and a tetrahedron in three-dimensional ones, $\vec{\nu}_{i,T} = \int_{\partial C_i(\mathrm{X})\cap T} \vec{n}d\sigma$, $\vec{n}$ is the normal to the cell boundary, and $\mathcal{R}(T) = \mathcal{R}(W)_{|T}$ is the constant value of $\mathcal{R}(W)$ over T obtained by computing the mean value of $\vec{v}$ over T as $\vec{v}(T) = \frac{1}{3}\sum_{k,\ k\in T} \vec{v}_k$ in two-dimensional problems, and $\vec{v}(T) = \frac{1}{4}\sum_{k,\ k\in T} \vec{v}_k$ in three-dimensional ones.

3 Time-accurate integration of the diffusive fluxes

Let Δt and $t^n = n\Delta t$ denote respectively the chosen time-step and the n-th time-station. Integrating Eq. (6) between t^n and t^{n+1} leads to

$$A_i(X^{n+1})W_i^{n+1} - A_i(X^n)W_i^n + \int_{t^n}^{t^{n+1}} F_i(W, X, \dot{X})dt \;=\; \int_{t^n}^{t^{n+1}} R_i(W, X)dt \qquad (8)$$

The proper evaluation of the integrals $\int_{t^n}^{t^{n+1}} F_i(W, X, \dot{X})dt$ *(i)* and $\int_{t^n}^{t^{n+1}} R_i(W, X)dt$ *(ii)* raises the question of where to integrate the fluxes: on the mesh configuration at (t^n, X^n), on that at (t^{n+1}, X^{n+1}), or in between these two configurations? In [7, 8], the authors have focused on Euler flows and have pointed out that any proposed method for evaluating the integral *(i)* must preserve the state W^* of a uniform flow. From this principle, they have derived a GCL as well as suitable explicit and implicit schemes for time-integrating the inviscid equivalent of Eq. (8). Unfortunately, setting in Eq. (8) $W_i^n = W_i^{n+1} = W_i^*$ annihilates the integral *(ii)*, and therefore does not indicate how to compute $\int_{t^n}^{t^{n+1}} R_i(W, X)dt$. Next, we address this specific issue, and derive a family of algorithms for computing $\int_{t^n}^{t^{n+1}} R_i(W, X)dt$ with a desirable accuracy.

3.1 The two-dimensional case

The discretized diffusive fluxes (7) can be written as

$$R_i(W, X) = \sum_{j\in\{i,V(i)\}} \sum_{T\in Supp(\phi_j)} \frac{1}{Area(T)}\, G_j(W, \vec{\nu}_{j,T}, \vec{\nu}_{i,T}) \qquad (9)$$

where $V(i)$ is the set of the neighbors of x_i, ϕ_j is the P_1 Galerkin function associated with x_j, $Supp(\phi_j) = \{T \;/\; \phi_j \neq 0 \text{ on } T\}$, $\vec{\nu}_{j,T} = \int_{\partial C_j(\mathrm{X})\cap T} \vec{n}d\sigma$, and G_j is a four-component vector given by

$$G_j(W, \vec{\nu}_{j,T}, \vec{\nu}_{i,T}) = -\frac{\mu}{Rey} \begin{pmatrix} G_{1j}(W, \vec{\nu}_{j,T}, \vec{\nu}_{i,T}) \\ G_{2j}(W, \vec{\nu}_{j,T}, \vec{\nu}_{i,T}) \end{pmatrix} .\vec{\nu}_{i,T}$$

where

$$\begin{pmatrix} G_{1j}^t(W, \vec{\nu}_{j,T}, \vec{\nu}_{i,T}) \\ G_{2j}^t(W, \vec{\nu}_{j,T}, \vec{\nu}_{i,T}) \end{pmatrix} =$$
$$\left(\vec{0}\;,\; \vec{r}(W_j, \vec{\nu}_{j,T}, \vec{e}_1)\;,\; \vec{r}(W_j, \vec{\nu}_{j,T}, \vec{e}_2)\;,\; \vec{r}(W_j, \vec{\nu}_{j,T}, \vec{v}(T)) + \frac{\gamma}{Pr} e_j \vec{\nu}_{j,T}\right)$$

In the above expression, $\vec{0} = (0, 0)^t$, and $\vec{r}$ is a two-component vector defined by

$$\vec{r}(W_j, \vec{\nu}_{j,T}, \vec{b}) = \left[M(\vec{v}_j) \otimes M^t(\vec{\nu}_{j,T}) + M^t(\vec{v}_j) \otimes M(\vec{\nu}_{j,T}) - \frac{2}{3}\vec{v}_j.\vec{\nu}_{j,T} I_d\right] .\vec{b}$$

where $\vec{b} \in I\!R^2$, and the following notation is used for $\vec{c} \in I\!R^2$ and $A,\ B \in I\!R^2 \times I\!R^2$

$$M(\vec{c}) = \begin{pmatrix} c_1 & c_1 \\ c_2 & c_2 \end{pmatrix} \quad \text{and} \quad (A \otimes B)_{ij} = A_{ij} \times B_{ij} \quad \text{for } i,j = 1,2 \quad .$$

We assume that within the time-interval $[t^n, t^{n+1}]$, the position of a grid point x_i can be described by the linear transformation

$$\begin{aligned} x_i(t) &= \delta(t) x_i^{n+1} + (1 - \delta(t)) x_i^n \\ \delta(t) &= \frac{t - t^n}{\Delta t} \quad . \end{aligned} \tag{10}$$

In that case, $\vec{\nu}_{i,T}$, $\vec{\nu}_{j,T}$ and $Area(T)$ can be expressed in terms of $\delta(t)$ and Δt as follows

$$\begin{aligned} \vec{\nu}_{i,T} &= \int_{\partial C_i(\mathrm{X}) \cap T} \vec{n} d\sigma = \tfrac{1}{2} H (x_j - x_k) = \tfrac{1}{2} H \left[\delta(t) \Delta t (\dot{x}_j - \dot{x}_k) + x_j^n - x_k^n \right] \\ \vec{\nu}_{j,T} &= \int_{\partial C_j(\mathrm{X}) \cap T} \vec{n} d\sigma = \tfrac{1}{2} H (x_k - x_i) = \tfrac{1}{2} H \left[\delta(t) \Delta t (\dot{x}_k - \dot{x}_i) + x_k^n - x_i^n \right] \end{aligned}$$

$$\begin{aligned} Area(T) &= \tfrac{1}{2} \left[P (x_j - x_i) \wedge P (x_k - x_i) \right] . \hat{z} \\ &= \tfrac{1}{2} \left[P \left(\delta(t) \Delta t (\dot{x}_j - \dot{x}_i) + x_j^n - x_i^n \right) \wedge P \left(\delta(t) \Delta t (\dot{x}_k - \dot{x}_i) + x_k^n - x_i^n \right) \right] . \hat{z} \end{aligned}$$

where $H = \begin{pmatrix} 0 & -1 \\ 1 & 0 \end{pmatrix}$, $P = \begin{pmatrix} 1 & 0 & 0 \\ 0 & 1 & 0 \end{pmatrix}^t$, $\dot{x} = \dfrac{x^{n+1} - x^n}{\Delta t}$, x_i, x_j and x_k are the three vertices defining triangle T and positioned as depicted in Fig. 3, and $\hat{z}$ is the unit vector along the Oz axis.

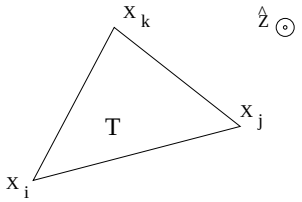

Figure 3: Description of a triangle T

Substituting the above expressions of $\vec{\nu}_{i,T}$, $\vec{\nu}_{j,T}$ and $Area(T)$ in Eq. (9), leads to

$$\int_{t^n}^{t^{n+1}} R_i(W,X) dt \ = \ \Delta t \int_0^1 \left(\sum_{k=0}^{2} a_k \Delta t^k \delta(t)^k \Big/ \sum_{k=0}^{2} b_k \Delta t^k \delta(t)^k \right) d\delta(t) \tag{11}$$

where a_k is some function of (X^n,$\dot{X}$,W), and b_k is a certain function of (X^n, $\dot{X}$).

Now, developing the integrand of integral (11) in a Taylor series in Δt gives

$$\int_{t^n}^{t^{n+1}} R_i(W,X) dt \ = \ \Delta t \int_0^1 (c_0 + c_1 \Delta t \delta(t) + c_2 \Delta t^2 \delta(t)^2 + \cdots) d\delta(t) \tag{12}$$

where c_k is another function of (X^n,$\dot{X}$,W).

Finally, depending on the quadrature rule chosen for evaluating the above integral, the following time-accuracy results are obtained

a) If the integration of Eq. (12) is performed at $\delta(t) = 0$, only the constant polynomials of $\delta(t)$ are computed exactly, so that

$$\begin{aligned} \int_{t^n}^{t^{n+1}} R_i(W,X)dt &= \Delta t R_i(W^k, X^n) + O(\Delta t^2) \\ k &= n \quad \text{for explicit schemes} \\ k &= n+1 \quad \text{for implicit schemes} \end{aligned}$$

b) If the midpoint rule is used for evaluating Eq. (12), the linear components of $\delta(t)$ are computed exactly, and therefore

$$\begin{aligned} \int_{t^n}^{t^{n+1}} R_i(W,X)dt &= \Delta t R_i(W^k, X^{n+\frac{1}{2}}) + O(\Delta t^3) \\ k &= n \quad \text{for explicit schemes} \\ k &= n+\tfrac{1}{2} \quad \text{for implicit schemes} \\ W^{n+\frac{1}{2}} &= \tfrac{W^{n+1}-W^n}{2} \\ X^{n+\frac{1}{2}} &= \tfrac{X^{n+1}-X^n}{2} \end{aligned}$$

c) On the other hand, if the two-point integration rule at $\delta(t) = \frac{1}{2} \mp \frac{1}{2\sqrt{3}}$ is used, the quadratic components of $\delta(t)$ are computed exactly, and one obtains

$$\begin{aligned} \int_{t^n}^{t^{n+1}} R_i(W,X)dt &= \frac{\Delta t}{2}\left[R_i(W^{k1}, X^{m_1}) + R_i(W^{k2}, x^{m_2})\right] + O(\Delta t^5) \\ m1 &= n + \tfrac{1}{2} - \tfrac{1}{2\sqrt{3}} \\ m2 &= n + \tfrac{1}{2} + \tfrac{1}{2\sqrt{3}} \\ k1 &= n \quad \text{for explicit schemes} \\ k2 &= n \quad \text{for explicit schemes} \\ k1 &= m1 \quad \text{for implicit schemes} \\ k2 &= m2 \quad \text{for implicit schemes} \\ W^{n+\beta} &= \beta W^{n+1} + (1-\beta)W^n \\ X^{n+\beta} &= \beta X^{n+1} + (1-\beta)X^n \end{aligned}$$

Hence, whether an explicit or implicit time-integration scheme $\mathcal{S}$ is chosen for solving the unsteady two-dimensional Navier-Stokes equations, the evaluation of $\int_{t^n}^{t^{n+1}} R_i(W,X)dt$ should be carried out on the configuration (t^n, X^n) if $\mathcal{S}$ is first-order accurate, on the midpoint configuration if $\mathcal{S}$ is second-order accurate, and using the two-point configuration if $\mathcal{S}$ is fourth-order accurate.

3.2 The three-dimensional case

For three-dimensional problems, the discretized diffusive fluxes (7) become

$$R_i(W,X) = \sum_{j\in\{i,V(i)\}} \sum_{T\in Supp(\phi_j)} \frac{1}{Vol(T)}\, G_j(W,\vec{\nu}_{j,T},\vec{\nu}_{i,T})$$

where $V(i)$, ϕ_j and $Supp(\phi_j)$ have the same meaning as in the two-dimensional case, T denotes a tetrahedron and $Vol(T)$ its volume, $\vec{\nu}_{j,T} = \int_{\partial C_j(\mathrm{X})\cap T} \vec{n} d\sigma$, and G_j is a five-component vector given by

$$G_j(W,\vec{\nu}_{j,T},\vec{\nu}_{i,T}) = -\frac{\mu}{Rey} \begin{pmatrix} G_{1j}(W,\vec{\nu}_{j,T},\vec{\nu}_{i,T}) \\ G_{2j}(\mathrm{W},\vec{\nu}_{j,T},\vec{\nu}_{i,T}) \\ G_{3j}(\mathrm{W},\vec{\nu}_{j,T},\vec{\nu}_{i,T}) \end{pmatrix} .\vec{\nu}_{i,T}$$

where

$$\begin{pmatrix} G^t_{1j}(\mathrm{W},\vec{\nu}_{j,T},\vec{\nu}_{i,T}) \\ G^t_{2j}(\mathrm{W},\vec{\nu}_{j,T},\vec{\nu}_{i,T}) \\ G^t_{3j}(\mathrm{W},\vec{\nu}_{j,T},\vec{\nu}_{i,T}) \end{pmatrix} =$$

$$\left(\vec{0}\ ,\ \vec{r}(\mathrm{W}_j,\vec{\nu}_{j,T},\vec{e}_1)\ ,\ \vec{r}(\mathrm{W}_j,\vec{\nu}_{j,T},\vec{e}_2)\ ,\ \vec{r}(\mathrm{W}_j,\vec{\nu}_{j,T},\vec{e}_3)\ ,\ \vec{r}(\mathrm{W}_j,\vec{\nu}_{j,T},\vec{v}(T)) + \frac{\gamma}{Pr} e_j \vec{\nu}_{j,T}\right)$$

In the above expression, $\vec{0} = (0,0,0)^t$, $\vec{e}_1 = (1,0,0)^t$, $\vec{e}_2 = (0,1,0)^t$, $\vec{e}_3 = (0,0,1)^t$, and $\vec{r}$ is a three-component vector defined by

$$\vec{r}(W_j,\vec{\nu}_{j,T},\vec{b}) = \left[M(\vec{v}_j)\otimes M^t(\vec{\nu}_{j,T}) + M^t(\vec{v}_j)\otimes M(\vec{\nu}_{j,T}) - \frac{2}{3}\vec{v}_j.\vec{\nu}_{j,T} I_d\right].\vec{b}$$

where $\vec{b}\in I\!R^3$, and the following notation is used for $\vec{c}\in I\!R^3$ and $A,\ B\in I\!R^3\times I\!R^3$

$$M(\vec{c}) = \begin{pmatrix} c_1 & c_1 & c_1 \\ c_2 & c_2 & c_2 \\ c_3 & c_3 & c_3 \end{pmatrix} \quad \text{and} \quad (A\otimes B)_{ij} = A_{ij}\times B_{ij} \quad \text{for } i,j = 1,\ldots,3 \quad .$$

Using the same parametrization (Fig. 4) as in the two-dimensional case for the evolution of a grid point during $[t^n, t^{n+1}]$ (given by (10)), we derive new expressions for $\vec{\nu}_{j,T}$, $\vec{\nu}_{i,T}$ and $Vol(T)$ as functions of $\delta(t)$ and Δt

$$\begin{aligned}
\vec{\nu}_{i,T} &= \int_{\partial C_i(\mathrm{X})\cap T} \vec{n} d\sigma \\
&= \tfrac{1}{6}(x_k - x_j)\wedge(x_l - x_j) \\
&= \tfrac{1}{6}\Big[\Big(\delta(t)\Delta t(\dot{x}_k - \dot{x}_j) + \mathrm{x}^n_k - x^n_j\Big)\wedge\Big(\delta(t)\Delta t(\dot{x}_l - \dot{x}_j) + x^n_l - x^n_j\Big)\Big] \\
\vec{\nu}_{j,T} &= \tfrac{1}{6}[(\delta(t)\Delta t(\dot{x}_l - \dot{x}_i) + x^n_l - x^n_i)\wedge(\delta(t)\Delta t(\dot{x}_k - \dot{x}_i) + x^n_k - x^n_i)] \\
Vol(T) &= \tfrac{1}{6}((x_k - x_j)\wedge(x_l - x_j)).(x_j - x_i) \\
&= \tfrac{1}{6}\Big[\Big(\delta(t)\Delta t(\dot{x}_k - \dot{x}_j) + x^n_k - x^n_j\Big)\wedge\Big(\delta(t)\Delta t(\dot{x}_l - \dot{x}_j) + x^n_l - x^n_j\Big)\Big] \\
&\quad .\Big(\delta(t)\Delta t(\dot{x}_j - \dot{x}_i) + x^n_j - x^n_i\Big)
\end{aligned}$$

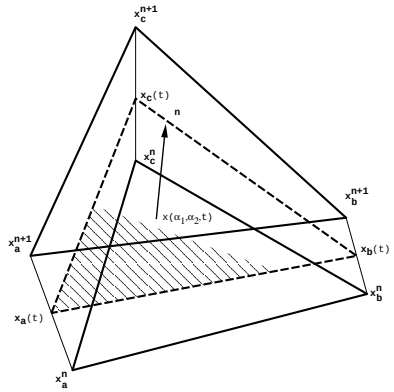

Figure 4: Parametrization of a facet in the three-dimensional case

where x_i, x_j, x_k and x_l are the four vertices defining the tetrahedron T and positioned as depicted in Fig. 5, and $\dot{x} = \dfrac{x^{n+1} - x^n}{\Delta t}$.

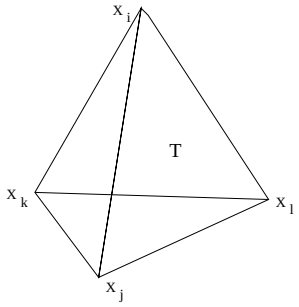

Figure 5: Description of a tetrahedron T

From the above expressions of $\vec{\nu}_{i,T}$, $\vec{\nu}_{j,T}$ and $Vol(T)$ we deduce

$$\int_{t^n}^{t^{n+1}} R_i(W,X)dt \;=\; \Delta t \int_0^1 \left(\sum_{k=0}^{4} a_k \Delta t^k \delta(t)^k \Big/ \sum_{k=0}^{3} b_k \Delta t^k \delta(t)^k \right) d\delta(t) \tag{13}$$

where a_k is a function of (X^n,$\dot{X}$,W), and b_k is a function of (X^n, $\dot{X}$).

As in the two-dimensional case, we develop the integrand of integral (13) in a Taylor series

$$\int_{t^n}^{t^{n+1}} R_i(W,X)dt \;=\; \Delta t \int_0^1 (c_0 + c_1 \Delta t \delta(t) + c_2 \Delta t^2 \delta(t)^2 + \cdots) d\delta(t) \tag{14}$$

where c_k is yet another function of (X^n,$\dot{X}$,W). Depending on the quadrature rule chosen for evaluating the above integral, we obtain the following time-accuracy results

a) If the integration of Eq. (14) is performed at $\delta(t) = 0$, only the constant polynomials of $\delta(t)$ are computed exactly, so that

$$\begin{aligned} \int_{t^n}^{t^{n+1}} R_i(W,X)dt &= \Delta t R_i(W^k, X^n) + O(\Delta t^2) \\ k &= n \quad \text{for explicit schemes} \\ k &= n+1 \quad \text{for implicit schemes} \end{aligned}$$

b) If the midpoint rule is used for evaluating Eq. (14), the linear components of $\delta(t)$ are computed exactly, and therefore

$$\begin{aligned} \int_{t^n}^{t^{n+1}} R_i(W,X)dt &= \Delta t R_i(W^k, X^{n+\frac{1}{2}}) + O(\Delta t^3) \\ k &= n \quad \text{for explicit schemes} \\ k &= n+\tfrac{1}{2} \quad \text{for implicit schemes} \\ W^{n+\frac{1}{2}} &= \tfrac{W^{n+1}-W^n}{2} \\ X^{n+\frac{1}{2}} &= \tfrac{X^{n+1}-X^n}{2} \end{aligned}$$

c) On the other hand, if the two-point integration rule at $\delta(t) = \frac{1}{2} \mp \frac{1}{2\sqrt{3}}$ is used, the quadratic components of $\delta(t)$ are computed exactly, and one obtains

$$\begin{aligned} \int_{t^n}^{t^{n+1}} R_i(W,X)dt &= \frac{\Delta t}{2}\left[R_i(W^{k1}, X^{m_1}) + R_i(W^{k2}, x^{m_2})\right] + O(\Delta t^5) \\ m1 &= n + \tfrac{1}{2} - \tfrac{1}{2\sqrt{3}} \\ m2 &= n + \tfrac{1}{2} + \tfrac{1}{2\sqrt{3}} \\ k1 &= n \quad \text{for explicit schemes} \\ k2 &= n \quad \text{for explicit schemes} \\ k1 &= m1 \quad \text{for implicit schemes} \\ k2 &= m2 \quad \text{for implicit schemes} \\ W^{n+\beta} &= \beta W^{n+1} + (1-\beta)W^n \\ X^{n+\beta} &= \beta X^{n+1} + (1-\beta)X^n \end{aligned}$$

Hence, whether an explicit or implicit time-integration scheme $\mathcal{S}$ is chosen for solving the unsteady three-dimensional Navier-Stokes equations, the evaluation of $\int_{t^n}^{t^{n+1}} R_i(W,X)dt$ should be carried out on the configuration (t^n, X^n) if $\mathcal{S}$ is first-order accurate, on the midpoint configuration if $\mathcal{S}$ is second-order accurate, and using the two-point configuration if $\mathcal{S}$ is fourth-order accurate.

4 Applications

Here, we illustrate the methodology described in this paper for computing the diffusive fluxes on dynamic meshes, with a three-dimensional viscous flow problem related to a supersonic aeroelastic application.

We consider the supersonic flow above a flexible panel of length $L_1 = 0.5$, width $L_2 = 0.1$, and thickness $th = 0.00135$. The panel is clamped at both ends. The flow domain is discretized into 20250 vertices and 94080 tetrahedra. The freestream Mach number is set to $M_\infty = 1.9$, the Reynolds number to $Rey = 100$, and the initial angle of attack to $\alpha = 0$.

The panel is forced to oscillate around its fundamental flexible mode shape X_P^1 with a constant circular frequency ω and an amplitude a (Fig 6). Hence, the position X_B of the fluid points lying on the surface of the panel are forced into the harmonic motion

$$X_B \; = \; aX_P^1 sin\omega t$$

The amplitude a is chosen so that the maximum vertical deflection of the panel is equal to 5.4% of its length L_1. The circular frequency is set to $\omega = 1000$. At each time-step t^n, the position of the fluid dynamic mesh is updated by a Jacobi-based relaxation scheme [3, 13] in order to conform to the new boundary position. Finally, we note that the CFD code employed in this investigation utilizes a first-order accurate backward Euler scheme for time-integrating the semi-discrete three-dimensional Navier-Stokes equations.

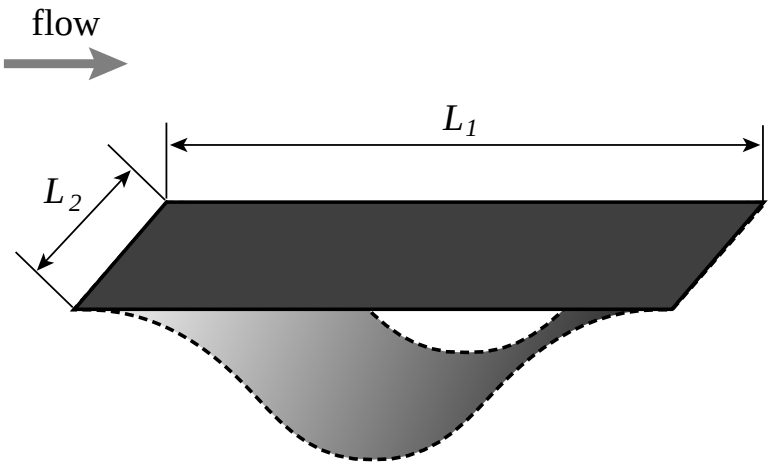

Figure 6: Oscillating panel

First, the CFL (Courant-Friedrichs-Lewy criterion) number is set to 10, and the diffusive fluxes are evaluated at the midpoint configuration (even though the backward Euler scheme is only first-order accurate). The resulting unsteady solution is labeled as the reference solution because at CFL=10, the period of the predicted lift is sampled at 500 time-steps. Next, the CFL number is set to 100, and two other unsteady solutions are computed, using the (t^n, X^n) and midpoint configurations for evaluating the diffusive fluxes, respectively. The computed lift histories are graphically depicted in Fig. (7).

Clearly, the results reported in Fig. (7) highlight the effect of the algorithm used for evaluating the diffusive fluxes on dynamic meshes, and its impact on the accuracy of the overall flow simulation. When the midpoint configuration (second-order time-accurate) is used instead of the (t^n, X^n) configuration (first-order time-accurate) for computing the viscous fluxes, the accuracy of the lift is improved by roughly 4%. More drastic improvements

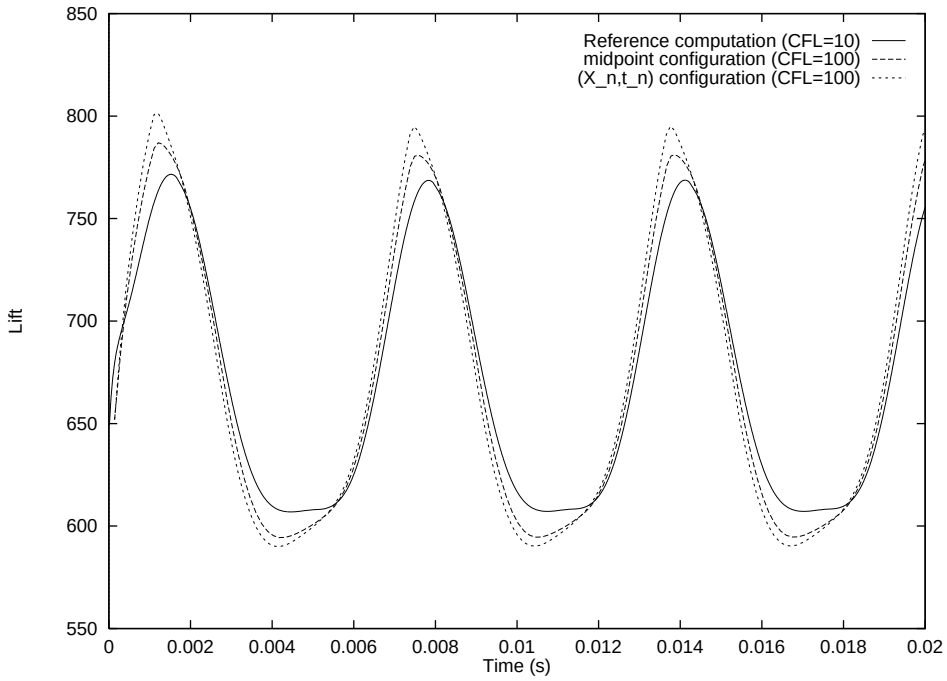

Figure 7: Lift prediction using various algorithms for evaluating the diffusive fluxes

can be expected when the semi-discrete Navier-Stokes equations are time-integrated with a second-order implicit scheme — which our current code does not have — because in that case larger time-steps can be afforded, and the errors resulting from computing the "moving" diffusive fluxes at the (t^n, X^n) configuration grow as $O(\Delta t)$, while those resulting from computing these fluxes at the midpoint configuration grow as $O(\Delta t^2)$.

5 Conclusion

In this paper, we have considered the solution of unsteady laminar viscous flow problems with moving boundaries and deformable dynamic meshes. We have presented a methodology for computing accurately the diffusive fluxes associated with such problems, and highlighted its impact on the overall accuracy of the flow simulation. The numerical schemes presented in this paper can be directly extended to the computation of turbulent flows on moving grids.

Acknowledgement

The first author acknowledges the support by a post-doctoral fellowship from the DRET. The second author acknowledges partial support by the National Science Foundation under grant ASC-9217394.

References

[1] H. Tijdman and R. Seebass, *Transonic Flow Past Oscillating Airfoils*, Ann. Rev. Fluid Mech. 1980, 12:181-222.

[2] J.W. Edwards and J.B. Malone, *Current Status of Computational Methods for Transonic Unsteady Aerodynamics and Aeroelastic Applications*, Comput. Sys. Engrg. 1992, 3:545-569.

[3] J.T. Batina, *Unsteady Euler Airfoil Solutions Using Unstructured Dynamic Meshes*, AIAA Paper 89-0115, AIAA 27th Aerospace Sciences Meeting, Reno, Nevada, January 9-12, 1989.

[4] J. Donea, *An Arbitrary Lagrangian-Eulerian Finite Element Method for Transient Fluid-Structure Interactions*, Comput. Meths. Appl. Mech. Engrg. 1982, 33: 689–723.

[5] C. Farhat, M. Lesoinne and N. Maman, *Mixed Explicit/Implicit Time Integration of Coupled Aeroelastic Problems: Three-Field Formulation, Geometric Conservation and Distributed Solution*, Internat. J. Numer. Meths. Fluids 1995, 21:807-835.

[6] J.A. Ekaterinaris and F.R. Menter, *Computation of Oscillating Airfoil Flows with One- and Two-Equation Turbulence Models*, AIAA J. 1994, 32: 2359-2365.

[7] M. Lesoinne and C. Farhat, *Geometric Conservation Laws for Aeroelastic Computations Using Unstructured Dynamic Meshes*, AIAA Paper 95-1709, 12th AIAA Computational Fluid Dynamics Conference, San Diego, June 19-22, 1995.

[8] M. Lesoinne and C. Farhat, *Geometric Conservation Laws for Flow Problems with Moving Boundaries and Deformable Meshes, and Their Impact on Aeroelastic Computations*, Comput. Meths. Appl. Mech. Engrg. (in press).

[9] P.D. Thomas and C. K. Lombard, *Geometric Conservation Law and its Application to Flow Computations on Moving Grids*, AIAA J. 1979, 17:1030-1037.

[10] W. K. Anderson, J. L. Thomas and C. L. Rumsey, *Extension and Application of Flux-Vector Splitting to Unsteady Calculations on Dynamic Meshes.* AIAA Paper 87-1152-CP, 1987.

[11] H. Zhang, M. Reggio, J.Y. Trépanier and R. Camarero, *Discrete Form of the GCL for Moving Meshes and its Implementation in CFD Schemes,* Comput. Fluids 1993, 22:9–23.

[12] B. NKonga and H. Guillard, *Godunov Type Method on Non-Structured Meshes for Three-Dimensional Moving Boundary Problems*, Comp. Meths. Appl. Mech. Engrg. 1994, 113:183-204.

[13] C. Farhat and S. Lantéri, *Simulation of Compressible Viscous Flows on a Variety of MPPs: Computational Algorithms for Unstructured Dynamic Meshes and Performance Results,* Comput. Meths. Appl. Mech. Engrg. 1994, 119:35-60.

Unité de recherche INRIA Lorraine, Technopôle de Nancy-Brabois, Campus scientifique,
615 rue du Jardin Botanique, BP 101, 54600 VILLERS LÈS NANCY
Unité de recherche INRIA Rennes, Irisa, Campus universitaire de Beaulieu, 35042 RENNES Cedex
Unité de recherche INRIA Rhône-Alpes, 46 avenue Félix Viallet, 38031 GRENOBLE Cedex 1
Unité de recherche INRIA Rocquencourt, Domaine de Voluceau, Rocquencourt, BP 105, 78153 LE CHESNAY Cedex
Unité de recherche INRIA Sophia-Antipolis, 2004 route des Lucioles, BP 93, 06902 SOPHIA-ANTIPOLIS Cedex

Éditeur
INRIA, Domaine de Voluceau, Rocquencourt, BP 105, 78153 LE CHESNAY Cedex (France)
ISSN 0249-6399